

Transport through a Kondo quantum dot: Functional RG approach

H. Schmidt¹ and P. Wölfle^{1,2}

¹ Institut für Theorie der Kondensierten Materie and DFG-Center for Functional Nanostructures, Universität Karlsruhe, 76128 Karlsruhe, Germany

² Institut für Nanotechnologie, Forschungszentrum Karlsruhe, 76021 Karlsruhe, Germany

Received 29 September 2009, revised 13 November 2009, accepted 19 November 2009 by U. Eckern

Key words Kondo dot model, electronic transport, functional renormalization group.

PACS 72.15.Qm, 73.63.Kv

We apply the functional renormalization group (FRG) method to calculate the conductance of a quantum dot in the Kondo regime. Starting from the exact FRG equations in Keldysh formulation for the Kondo exchange Hamiltonian in pseudo-fermion (pf) representation, we solve the coupled equations for the pf self energy and the coupling function, neglecting three-particle and higher correlation functions. The conductance G as a function of temperature T and bias voltage V is calculated using a renormalized Golden Rule expression. The limiting behavior at T and/or $V \ll T_K$ (T_K : Kondo temperature) agrees with known results. The difficulties when approaching strong coupling are analyzed and improvements are suggested.

1 Introduction

The Kondo effect is a ubiquitous phenomenon in the area of electron transport in nanostructures [1, 2, 3, 4, 5, 6]. For its existence a small system with internal degrees of freedom (e.g. a quantum dot with spin), coupled to a sufficiently large conduction electron system (the leads) is required. If certain symmetries are satisfied, the localized spin forms a resonance state with the surrounding conduction electron spins at the Fermi level, of energy width T_K , the Kondo temperature (here and in the following we use units where Boltzmann's constant $k_B = 1$ and Planck's constant $\hbar = 1$). A finite bias voltage V applied across the quantum dot is known to destroy the Kondo resonance, provided $eV \gg T_K$. It has been argued that the limitation in the coherence time brought about by inelastic processes in the leads causes the suppression of the Kondo effect at finite V ; since it cuts off the renormalization group flow of the coupling constant [8, 7]. At sufficiently large V this cutoff is still within the perturbative regime. In that case the perturbative RG treatment ("poor man's scaling", [9]) generalized to nonequilibrium, proposed in [10], provides a controlled and complete description of all physical quantities. Indeed the latter theory has been used to describe experimental data for various situations, each time with excellent success [11, 12, 13, 14]. While the effect of decoherence on the RG flow of the coupling constant has been included in [10, 11] in a phenomenological way, it is of interest to derive the effect of the decoherence rate in a systematic fashion. The way in which the decoherence rate cuts off the logarithmic singularities in perturbation theory has been analyzed in [30], where it has been found that the decoherence appears in the form of physically accessible rates, namely the longitudinal and transverse spin relaxation rates. In a completely new way the effect of decoherence on the Kondo effect has been analyzed within the flow equation method [15], with results in agreement with and thus confirming the work by Paaske et al. [10, 30]. The latter method is, however, not

Corresponding author E-mail: woelfle@tkm.uni-karlsruhe.de, Phone: +49 721 608 3590

easily applicable to the calculation of observable quantities like the conductance. It is therefore worthwhile to work out a systematic and consistent derivation of the coupled RG-equations for the coupling function and the decoherence rate, even in the weak coupling regime.

On the other hand, it has not been possible, so far, to calculate the influence of a finite bias voltage in the strong coupling regime. There are several methods available describing properties of the Kondo system at strong coupling in equilibrium (see [16]), but a general and practically applicable extension of these methods to nonequilibrium has not been found yet. A recently proposed "Conserving T-matrix approximation", based on self-consistent renormalized perturbation theory including all two-particle channels, which has been shown to recover correctly the Fermi liquid behavior at low energies and the crossover to the local moment regime [17, 18], may in principle be generalized to nonequilibrium, but is at present too costly in numerical evaluation effort.

In this paper we present results for the weak-coupling regime of the Kondo model in and out of equilibrium obtained by the functional renormalization group (FRG) method [19, 20, 21, 22]. The FRG is a powerful tool when dealing with the diversity of energy scales and the interplay of correlations in an interacting fermionic systems such as the Kondo model where the microscopic energy scale band width D and the dynamically generated energy scale Kondo temperature T_K differ by orders of magnitude. The FRG uses an exact mapping of the initial model to models with reduced band width. The mapping generates an infinite hierarchy of flow equations, describing the gradual evolution from a microscopic model Hamiltonian to the effective action as a function of a continuously decreasing energy cutoff. In practice, one modifies the bare propagator by cutting off frequencies smaller than some infrared cutoff Λ . As this cutoff is progressively lowered more and more low-energy degrees of freedom are included, until the original model is recovered for $\Lambda \rightarrow 0$. The conventionally used approximation consists of a suitable truncation of the hierarchy of equations. We find that the truncation neglecting three particle and higher order correlation functions, and keeping only the self energy together with the four-point vertex function captures the weak coupling regime ($T \ll T_K$) completely. In this paper we show in detail how the transport properties of a Kondo quantum dot in the weak-coupling regime may be calculated in a systematic and complete way.

Compared to previous applications of the FRG method to Kondo physics ([23] and ref. therein) our approach differs in at least two ways: (1) the present work addresses the Kondo model, rather than the Anderson model (compare, however, the recent work [24] in which the dynamical spin response of the Kondo model has been considered, using a real-time RG method [33]); (2) in contrast to previous FRG works we include the effect of the decoherence rate.

2 Model and FRG formalism

We consider the model of a quantum dot described by a spin $\frac{1}{2}$ operator S coupled by exchange interaction and tunneling to the conduction electron spins as described by the Hamiltonian

$$H = \sum_k \epsilon_k c_k^\dagger c_k + J \sum_{\alpha=1,2} S_\alpha \cdot s_\alpha$$

Here ϵ_k ; $\alpha = 1, 2$ labels the leads assumed to be in equilibrium at chemical potentials $\mu_{1,2} = \mu \pm eV/2$ and $\alpha = \uparrow, \downarrow$ are spin indices. The conduction electron spin density operators at the quantum dot are defined as $s_\alpha = \sum_{k;\uparrow,\downarrow} \frac{1}{2} c_k^\dagger \sigma_\alpha c_k$, with c_k^\dagger an electron creation operator in momentum state k , lead α and spin state σ_α and the vector of Pauli matrices. The \mathbb{S}_α are tunneling operators for $\alpha = \uparrow, \downarrow$. We use a pseudo-fermion representation for the local spin $S = \frac{1}{2} \sum_{\sigma,\sigma'} f^\dagger_\sigma \sigma f_{\sigma'}$, with projection onto the physical Hilbert space by adding a term $\sum_{\sigma} f^\dagger_\sigma f_\sigma - 1$ to the Hamiltonian and taking the limit $\lambda \rightarrow 1$ (cf. [25, 26]).

The FRG equations for the self energy and the one-particle irreducible Green's functions are derived by mapping the generating functional for the connected Green's functions in Keldysh space (see [20, 21, 22,

23] for an introduction into the FRG method)

$$Z[\phi; \psi] = \int \mathcal{D}[\phi; \psi] \exp[iS[\phi; \psi] + (\phi; \psi) + h\phi; \psi]$$

with the action

$$S = (\phi; G_0^{-1} \phi) + (\psi; F_0^{-1} \psi) + V[\phi; \psi]$$

where G_0 and F_0 are the free propagator Keldysh matrices for the lead electrons and pseudo fermions, respectively, and $V[\phi; \psi]$ denotes the exchange interaction, onto a generating functional in which certain high energy degrees of freedom have been removed at the expense of changing the interaction part accordingly. We use standard notation for the functional integrals (see e.g. [27]). In particular all time integrals are extended over the Schwinger double time contour.

Since the interaction is local in space we may integrate out spatial degrees of freedom. Thus, for stationary situations, the propagators depend only on a single frequency. We choose to remove the high energy components of the lead electrons, by introducing a sharp and symmetric—with respect to ω —cutoff ω_c , expressed by the step function $\Theta(\omega_c - |\omega|)$, according to

$$G^{0; \omega}(\omega) = G^0(\omega) \Theta(\omega_c - |\omega|)$$

and resulting in a ω -dependent generating functional Z . It is convenient to perform a Legendre transformation to the generating functional \bar{W} for the one-particle irreducible (1PI) n -particle vertex functions Γ_n . An expansion of the functional \bar{W} in the fields Γ_n leads to the flow equations for the Γ_n , and in particular for the self energy (we use Σ instead of Γ_1):

$$\partial_t \Gamma_{ab}^{cd}(\omega) = \frac{1}{2} \text{P} \int_{\omega; \omega'; \omega''} \text{P} \int_{\omega'''} G^{0; \omega; \omega'}(\omega) \Gamma_{a; b}^{c; d}(\omega; \omega'; \omega''; \omega''') \quad (1)$$

and for the two-particle vertex function Γ_2 :

$$\begin{aligned} \partial_t \Gamma_{a; b}^{c; d}(\omega; \omega'; \omega''; \omega''') &= \frac{1}{2} \sum_{\omega'''} \Gamma_{a; a'}^{c; c'} G_n^{0; \omega; \omega'}(\omega) F^{b'a''}(\omega; \omega' + \omega''; \omega''') \Gamma_{b''; b'''}^{d''; d'''} \\ &+ \Gamma_{a; a'}^{d''; d'''} G_n^{0; \omega; \omega'}(\omega) F^{b'a''}(\omega; \omega' + \omega''; \omega''') \Gamma_{b''; b'''}^{c''; c'''} \end{aligned} \quad (2)$$

For the sake of simplicity we occasionally omit the frequency arguments of the vertex function. Keldysh indices are denoted by the latin indices $a; b; c; d$. At this stage we have already neglected the term in equ. (2) which involves the three particle vertex function Γ_3 . This term would obey the next RG equation in the infinite hierarchy of equations for the Γ_n . The principal approximation of our approach is the neglect of Γ_3 and all higher vertex functions. In Fig. 1 the flow equations (1) and (2) are depicted graphically. The boundary conditions at the initial value $t = 0 = D_0$ are given by

$$\Gamma_{ab}^{cd}(\omega) = 0 \quad (3)$$

$$\Gamma_{a; b}^{c; d}(\omega; \omega'; \omega''; \omega''') = \frac{1}{4} \text{J} \sim \omega \sim \omega' \sim \omega'' \sim \omega''' \quad (4)$$

independent of frequency. Here, Γ_{ab}^{cd} denotes the bare Keldysh vertex structure, which is given by

$$\Gamma_{ab}^{cd} = (\Gamma_{ab}^{cd})^{\bar{a}+1} \quad \text{or} \quad \Gamma_{ab}^{cd} = \frac{1}{2} (\Gamma_{ab}^{cd} + \Gamma_{ab}^{cd}) \quad (5)$$

in the contour ordered or the Keldysh rotated representation, respectively. Furthermore we use either a representation of the Keldysh matrices in the usual Schwinger contour ordered representation ($T; T^<; T^>$)

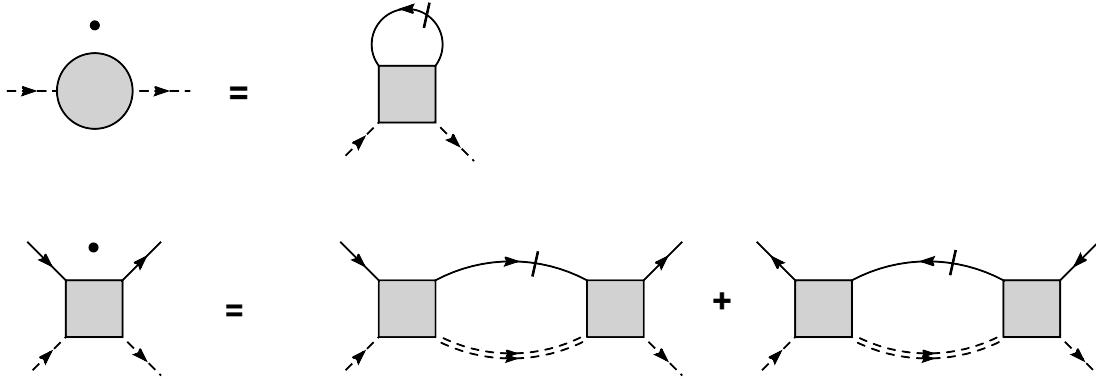


Fig. 1 Graphical representation of the fRG equation for the self energy and the two-particle vertex function as given by equ. (1) and (2). The dot on the l.h.s. represent the derivative w.r.t. λ . Solid lines with a stroke display the lead electrons propagator single scale propagator $S = G^0; \frac{d}{d\lambda} (G^0;)^{-1} G^0;$, whereas the double dashed lines represent the dressed pseudo-fermion propagator.

or in terms of retarded, advanced and Keldysh components (R ;A ;K), respectively. In both representations the matrix Green's functions are given by [28]

$$G = \begin{pmatrix} G^T & G^< \\ G^> & G^T \end{pmatrix} \quad \text{or} \quad G = \begin{pmatrix} G^R & G^K \\ 0 & G^A \end{pmatrix} \quad (6)$$

Corresponding representations are used for the pseudo-fermion self energies. The bare conduction electron local Green's functions at the quantum dot in both leads are given by

$$\begin{aligned} G^{0;R}(\omega) &= i N_0 (D_0 - \omega) = G^{0;A}(\omega) \\ G^{0;K}(\omega) &= 2i \tanh \frac{\omega}{2T} N_0 (D_0 - \omega) \\ G^{0;<}(\omega) &= i2 f(\omega) N_0 (D_0 - \omega) \\ G^{0;>}(\omega) &= i2 (1 - f(\omega)) N_0 (D_0 - \omega) \end{aligned}$$

where $N_0 = 1/2D_0$ is the density of states, $f(\omega) = 1/(\exp(\omega/T) + 1)$ is the Fermi function. Since we do not include a Zeeman term for the conduction electrons, the lead electron Green functions do not depend on spin and hence the spin indices have been suppressed. The dressed pseudo-fermion Green's functions read

$$\begin{aligned} F^R;(\omega) &= \frac{1}{i - \Sigma^R(\omega)} = F^A;(\omega) \\ F^K;(\omega) &= iA;(\omega)(1 - 2n;(\omega)) \\ F^<;(\omega) &= in;(\omega)A;(\omega) \\ F^>;(\omega) &= i(1 - n;(\omega))A;(\omega) \end{aligned}$$

with the spectral function

$$A;(\omega) = \frac{\Gamma(\omega)}{[\Gamma + \frac{\Sigma^R(\omega)}{2}]^2 + [\text{Im}(\Sigma^R(\omega))]^2} : \quad (7)$$

Here the imaginary part and the real part of the pseudo-fermion self energy are given by $\Sigma = i(\text{Im} \Sigma^R)$ or $\text{Re} \Sigma = \text{Re}(\text{Im} \Sigma^R)$, respectively. The pseudo-fermion occupation numbers are denoted by n_{σ} . Note that $n_{\sigma} \rightarrow 0$ in the limit $\beta \rightarrow \infty$ (compare the calculation of Σ in [26]). In the presence of a magnetic field, however, it is necessary to keep the n_{σ} , as they describe the local spin polarization $m = \lim_{\beta \rightarrow \infty} \frac{1}{\beta} \langle \sum_{\sigma} \sigma n_{\sigma} \rangle$.

3 FRG method applied to the Kondo model

3.1 Vertex function structure

Within the perturbative RG method as formulated in [10, 11] only a single component of Γ in Keldysh space has been kept. We now consider the structure of the vertex function Γ in Keldysh space in more detail. Starting point for the following considerations is equ. (2) in the Keldysh rotated form. The leading logarithmic terms in the FRG equation for the vertex function originate from the product of the Keldysh component of the lead electron Green function G^K with the real part of the retarded or advanced pseudo fermion propagator $F^{R/A}$. Keeping only these terms in the sum over Keldysh indices on the right hand side of equ. (2) and neglecting the ω dependence in the energy arguments of the vertex function this equation may be written in a short hand notation (keeping only Keldysh indices) as

$$\partial_{ab} \Gamma_{ab}^{cd} = \frac{1}{2} \sum_{a_0=1;2} \left[C_{R/A}^K \Gamma_{aa_0}^{1d} \Gamma_{a_0b}^{c2} + C_{R/A}^K \Gamma_{aa_0}^{c2} \Gamma_{a_0b}^{1d} \right] \quad (8)$$

Here C and C denote the kernels in the Peierls and the Cooper channel, respectively, and the leading components derive from its imaginary parts. For completeness, however, we state both the imaginary as well as the real parts. To this end we decompose the individual channels as

$$C_{R/A}^K = C_r + iC_i \quad (9)$$

$$\Gamma_{R/A}^K = \Gamma_r + i\Gamma_i; \quad (10)$$

with

$$\frac{C_i}{2N_0} = \sum_{\sigma} \frac{\tanh(\frac{\beta}{2T})(n_{\sigma}^f + n_{\sigma}^e + \frac{\beta}{2})}{(n_{\sigma}^f + n_{\sigma}^e + \frac{\beta}{2})^2 + \frac{\beta}{2}} \quad (11)$$

$$\frac{\Gamma_i}{2N_0} = \sum_{\sigma} \frac{\tanh(\frac{\beta}{2T})(n_{\sigma}^f + n_{\sigma}^e + \frac{\beta}{2})}{(n_{\sigma}^f + n_{\sigma}^e + \frac{\beta}{2})^2 + \frac{\beta}{2}} \quad (12)$$

and

$$\frac{C_r}{N_0} = \sum_{\sigma} \frac{\tanh(\frac{\beta}{2T})}{(n_{\sigma}^f + n_{\sigma}^e + \frac{\beta}{2})^2 + \frac{\beta}{2}} \quad (13)$$

$$\frac{\Gamma_r}{N_0} = \sum_{\sigma} \frac{\tanh(\frac{\beta}{2T})}{(n_{\sigma}^f + n_{\sigma}^e + \frac{\beta}{2})^2 + \frac{\beta}{2}} \quad (14)$$

To simplify matters we have already assumed an energy independent imaginary part of the pseudo fermion self energy and furthermore dropped the real part of the self energy. Again we emphasize that $C_i; \Gamma_i / \frac{1}{2}$ and hence produce the leading logarithmic components, whereas $C_r; \Gamma_r / \frac{1}{2}$ give rise to sub-leading

corrections. In the following we neglect contributions from C_r and C_l and focus on the leading components only. Hence, we are led to the equation

$$\textcircled{e} \Gamma_{ab}^{cd} = \frac{1}{2} \sum_{a \neq 1; 2} \sum_i \Gamma_{aa0}^{1d} \Gamma_{a0b}^{c2} + C_i \sum_{a \neq 1; 2} \sum_{\#} \Gamma_{aa0}^{c2} \Gamma_{a0b}^{1d} : \quad (15)$$

To examine the behaviour under the FRG we perform a Picard-Lindelöf like iteration, i.e. we start with the bare vertex structure $\Gamma_{ab}^{cd} = \Gamma_{ab}^{cd} = \frac{1}{2} \Gamma_{ab}^{1d} + \frac{1}{2} \Gamma_{ab}^{c2}$ on the right hand side of equ. (15). By performing the sum over Keldysh indices we see that in both the Cooper and Peierls channels this structure is reproduced. Hence, in leading order there is only one invariant amplitude, of the structure of the bare vertex

$$\Gamma_{ab}^{cd} = \Gamma_{ab}^{cd} : \quad (16)$$

confirming the treatment in [10, 11]. To recover the perturbative RG scheme of [10, 11] from the FRG equation (2) the following additional steps have to be performed: As a first step the imaginary part of the pseudo fermion self energy is neglected in the denominator of equ. (11) and (12). Moreover the energies of the pseudo fermions are put on-shell, i.e. $\epsilon_f = \epsilon_B = 2$. Then the coupling function depends only on a single frequency, the frequency of the incoming electron. Finally the cutoff dependences in the Cooper and Peierls channels (equ. (11) and (12)) are approximated by a window function

$$\sum_{\#} \frac{\text{sign}(\epsilon)}{\epsilon!} = 2 \frac{1}{\epsilon!} \frac{1}{(\epsilon!)^2} \frac{1}{2} (\epsilon!)^2 \quad (17)$$

as described in more detail in [10, 11]. Here $\epsilon!$ depends on $v; B$ and the incoming and outgoing frequencies. Finally, in order to incorporate decoherence effects, which serve as a cutoff for the RG flow, a relaxation rate γ , which has contributions from both **pseudo fermion self energy and vertex corrections**, is incorporated in equ. (17) by replacing $(\epsilon!)^2$ by $(\epsilon!)^2 + \gamma^2$, where γ in turn is calculated by a second order golden rule expression with renormalized vertices. These two equations (i.e. for the coupling function and the decoherence rate γ) are then solved iteratively, until convergence is reached.

In the following we will show how the decoherence rate (to be more precise the imaginary part of the pseudo fermion self energy, which is part of the decoherence rate) arises in a natural way. To this end we first simplify the coupled equations (1) and (2) in an appropriate way and then solve these equations for different parameter regimes.

3.2 Approximated flow equations

In order to simplify the *coupled* differential equations for the imaginary part of the pseudo fermion self energy Σ and the effective interaction Γ we first neglect the frequency dependence of the leading component of Γ ,

$$\textcircled{e} \Gamma_{i_0}^{i_0} = \frac{1}{2} \sum_{\#} \Gamma_{i_0}^{i_0} \Gamma_{i_0}^{i_0} C(\epsilon) + \Gamma_{i_0}^{i_0} \Gamma_{i_0}^{i_0}(\epsilon) ; \quad (18)$$

where

$$C(\epsilon) = \frac{1}{2} \sum_{N_0} \frac{\tanh(\frac{\epsilon}{2T}) (\epsilon + \frac{B}{2})}{(\epsilon + \frac{B}{2})^2 + \frac{1}{2}} \quad (19)$$

$$\Gamma_{i_0}^{i_0}(\epsilon) = \frac{1}{2} \sum_{N_0} \frac{\tanh(\frac{\epsilon}{2T}) (\epsilon + \frac{B}{2})}{(\epsilon + \frac{B}{2})^2 + \frac{1}{2}} : \quad (20)$$

The RG equation for the imaginary part of the pseudo fermion self energy $\Sigma = i(\text{R} \quad \text{A})$ requires knowledge of the vertex function $\Gamma_{a;b}^{c;d}(\omega; \omega; \omega)$ at $\omega = 0$. By simply replacing this vertex function by an energy independent one of the form (16) the imaginary part of the pseudo fermion self energy is seen to vanish identically. Here it is necessary to take into account the subleading Keldysh components of Γ . To this end we use the leading components on the right hand side of the equation for $\Gamma(\omega; \omega; \omega)$, equ. (8), to generate the subleading Keldysh components, which we denote by $\mathbb{F}(\omega)$:

$$\textcircled{a} \quad \mathbb{F}_{a;b}^{c;d}(\omega) = \frac{1}{2} \frac{\hbar}{\omega} \left[\Gamma_{a;b}^{c;d}(\omega; \omega; \omega) + \Gamma_{aa^0}^{cc^0} \frac{d^0 d^0}{b^0 b^0} C_{aa^0 b^0 b^0}^{c^0 d^0}(\omega; \omega) + \Gamma_{a^0 b^0}^{c^0 d^0}(\omega; \omega) + \Gamma_{aa^0}^{d^0 d^0} \frac{cc^0}{b^0 b^0} \sim C_{aa^0 b^0 b^0}^{c^0 d^0}(\omega; \omega) \right] \quad (21)$$

where the Einstein summation convention is used. The kernels in the Cooper and Peierls channel read

$$C_{aa^0 b^0 b^0}^{c^0 d^0}(\omega; \omega) = \sum_{\sim} G^{d^0 c^0}(\sim) F^{b^0 a^0}(\omega - \sim) \quad (22)$$

$$\sim C_{aa^0 b^0 b^0}^{c^0 d^0}(\omega; \omega) = \sum_{\sim} G^{d^0 c^0}(\sim) F^{b^0 a^0}(\omega + \sim) : \quad (23)$$

With the aid of (21) the equation for the imaginary part of the pseudo fermion self energy may be cast in the form

$$\textcircled{a} \quad \Sigma = \frac{i}{2} \sum_{\sim} \mathbb{F}_{1;1}^{c;1}(\omega) \mathbb{F}_{2;2}^{c;2}(\omega) G^{cd}(\omega) \quad (24)$$

Hence equ. (18), (21) and (24) provide the desired system of coupled differential equations for the vertex function and the imaginary part of the pseudo fermion self energy. For the subsequent analysis we are going to use dimensionless couplings $g = N_0 I$. Additionally, the spin dependence of the vertex function is parameterized as $g_{\sigma}^{\sigma} = g_{\sigma}^{\sigma}$ and, for the sake of simplicity we restrict ourselves to the case of symmetric couplings $g_{\sigma}^{\sigma} = g$. Furthermore, in order to establish a more direct connection to Poor man's RG schemes [10, 11, 9] and to prevent a factor of i from pervading the formulas, we employ a redefinition of g , i.e. $g \rightarrow i8g$, which results in the new boundary condition $g = g_0 = N_0 J$ at $\omega = D_0$.

3.3 Weak coupling and linear response at finite temperature

To begin with a quantitative analysis we focus on the weak coupling regime $B; V \ll 0$ and $T = T_K \ll 1$, where the Kondo temperature is defined by $T_K = D_0 \exp(-1/(2g))$. In this case the Cooper and Peierls kernels (19) and (20) simplify to

$$C(\omega) = 4 N_0 \frac{\tanh(\frac{\omega}{2T})}{2 + (\omega/2)^2} = \quad (25)$$

Performing the internal spin sums in equ. (18), one finds

$$\textcircled{a} \quad g = 2g^2 \tanh \frac{\omega}{2T} \frac{1}{2 + \frac{\omega^2}{2}} ; \quad (26)$$

Similarly, in the absence of a magnetic field the RG equations for Σ and g take the simpler form

$$\textcircled{a} \quad \Sigma(\omega) = 3g^2 \sum_{\sim} f(\sim) \frac{1}{(\omega - \sim)^2 + (\omega/2)^2} \quad (27)$$

$$\textcircled{a} \quad \frac{dg}{d\omega} = \sum_{\sim} f(\sim) g(\sim) : \quad (28)$$

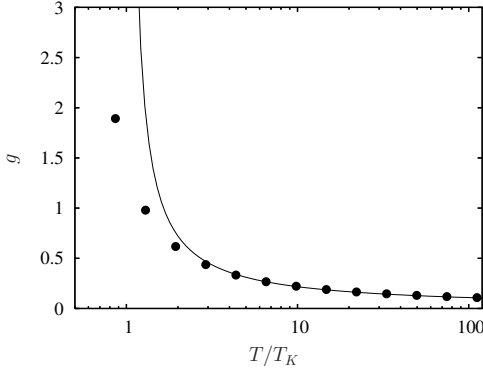


Fig. 2 Leading component of the coupling function $g(0)$ as a function of $T=T_K$ for values down to $T=T_K = 1$. Dots: results from FRG; solid line: $g = \frac{1}{2 \log(T=T_K)}$.

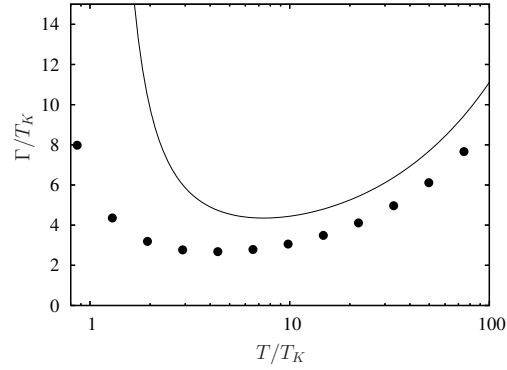


Fig. 3 Imaginary part of the self energy $\Gamma(0)$ versus $T=T_K$ for values down to $T=T_K = 1$. Dots: numerical results from FRG; solid line: $\Gamma = \frac{3}{2} T \frac{1}{(\log(T=T_K))^2}$.

In this case the corresponding initial conditions read

$$\mathfrak{g}^{0=D}(\epsilon) = 0 \quad \text{and} \quad \Gamma^{0=D} = 0 : \quad (29)$$

For the numerical treatment of these equations, however, we have to take a small but finite value for $\mathfrak{g}^{0=D}$. It turns out that the solution of the FRG equations does not depend much on the choice of the initial value of $\mathfrak{g}^{0=D}$ as long as it is taken to be sufficiently small.

We now solve the FRG equations for values of $T=T_K = 1$ and obtain results shown in Fig. 2 and Fig. 3. In Fig. 2 the leading Keldysh component of the coupling at the Fermi energy, $g(\epsilon = 0)$, is shown at zero bias as a function of $T=T_K$: At temperatures $T = T_K$ the numerical result (dots) agrees very well with the result of renormalized perturbation theory, $g = 1/2 \ln(T=T_K)$. It is seen that the effect of spin relaxation leads to a reduction of the growth of $g(\epsilon = 0)$ as compared to the weak coupling result, as expected, but does not cause $g(\epsilon = 0)$ to take a temperature independent value of order unity at $T = T_K$. The relaxation rate Γ , shown in Fig. 3, also agrees well with the renormalized perturbation theory expression, $\Gamma = 3/2 T \ln(T=T_K)^2$ at $T = T_K$. At lower temperatures Γ is seen to fall well below the diverging perturbative result, as expected, but does not appear to approach a limiting constant value of order T_K at $T = T_K$.

The conductance G (in units of e^2/h), in the absence of a magnetic field, may be approximately obtained from the golden rule expression

$$G(T) = \frac{3}{4} g^2(\epsilon = 0) \quad (30)$$

Fig. 4 shows a comparison of the linear conductance as obtained from equ. (30) (dots) and the weak coupling result (solid line) $G = (3/4) \ln(T=T_K)^2$. Even though the rapid rise of G as T approaches T_K is somewhat slowed down by the effect of the relaxation rate Γ , the slowdown is too weak or happens too late so that G rises beyond the unitarity limit.

It is somewhat surprising that the initial strong growth of g is not cut off more effectively by Γ . After all, at $T \approx T_K$ the relaxation rate reaches values of $\Gamma \approx 3T_K$ so that it might be expected to be more important than the temperature in cutting off the RG flow. The reason for this different behavior is apparent from Fig. 5 which shows the behavior of Γ as a function of the RG cutoff scale Λ : A sizeable value of Γ is only generated at the scale $\Lambda = T$ and not at T_K as one might have expected. Therefore, at $T = T_K$ and $\Lambda \approx T_K$ the relaxation width Γ is still exponentially small and does not serve to cut off the flow of g to large values, which explains why g ; Γ and G (at $\epsilon = 0$) appear to grow beyond the unitarity limit. We

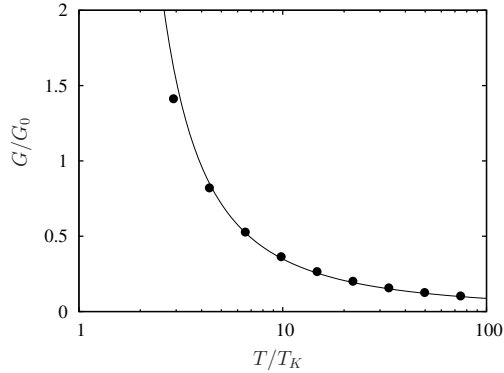


Fig. 4 Conductance in units of $G_0 = 2e^2/h$ versus $T=T_K$. Dots: numerical results from FRG; solid line: $G = G_0 = \frac{3}{16} \frac{2}{\log^2(T=T_K)}$.

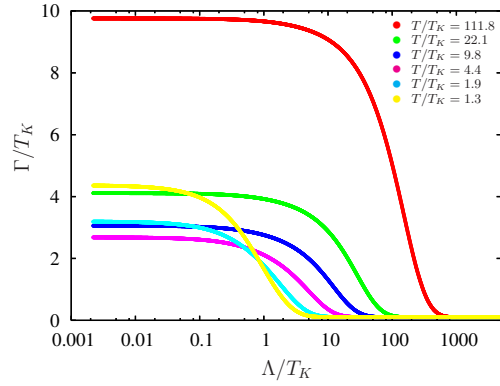


Fig. 5 FRG-flow of Γ for various values of $T=T_K$.

emphasize again that the above results depend sensitively on the approximation of neglecting the energy dependence, both, of the coupling function $g(\omega)$ and the relaxation rate $\Gamma(\omega)$ (see below).

3.4 Weak coupling at finite bias voltage

As it is known [10, 11] that in case of a finite bias voltage V the frequency dependence of the coupling function is crucial, in the following analysis we follow [10, 11] and maintain the frequency of the lead electron. We approximate the kernels in the Peierls and Cooper channels by using

$$\chi_{\pm} = \frac{\tanh(\frac{\omega}{2T})}{(\omega \pm 2)^2 + (\Gamma \pm 2)^2} \quad \text{and} \quad \rho = \frac{1}{(\omega)^2 + (\Gamma = 2)^2} \quad (31)$$

where $\Gamma = \Gamma(\omega)$. Hence, the equations for the leading component of the vertex function, $g(\omega)$, the subleading vertex component \mathfrak{g} , and the imaginary part of the pseudo fermion self energy take the form

$$\partial_{\omega} g(\omega) = -g^2(\omega) \chi_{\pm} \quad \text{and} \quad \rho = \frac{1}{(\omega)^2 + (\Gamma = 2)^2} \quad (32)$$

$$\partial_{\omega} \mathfrak{g}(\omega) = \frac{3}{2} g^2(0) \chi_{\pm} \chi_{\pm} f(\omega) \quad (33)$$

$$\partial_{\omega} \Gamma = \frac{1}{2} \chi_{\pm} \chi_{\pm} f(\omega) \mathfrak{g}(\omega); \quad (34)$$

where

$$f(\omega) = \frac{1}{\exp(\frac{\omega}{T}) + 1}; \quad \Gamma = eV = 2;$$

Results of a numerical solution of these RG equations are shown in Fig. 6 and Fig. 7. In Fig. 6 we display $g(\omega)$ for various values of $V=T_K$. Fig. 7 shows the imaginary part of the pseudo fermion self energy (dots) with the approximate expression $\Gamma = \frac{3}{4} V \frac{1}{\log^2(V=2T_K)}$ (solid line), which is seen to agree very well

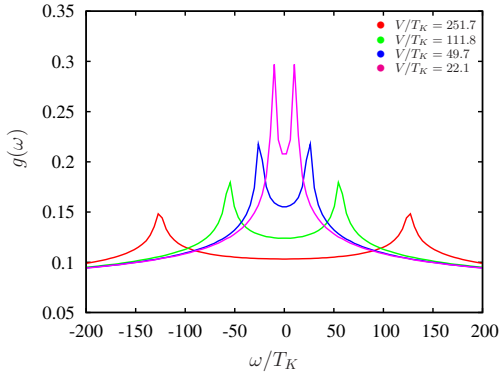


Fig. 6 Leading component of the coupling function $g(\omega)$ versus ω/T_K for various values of V/T_K .

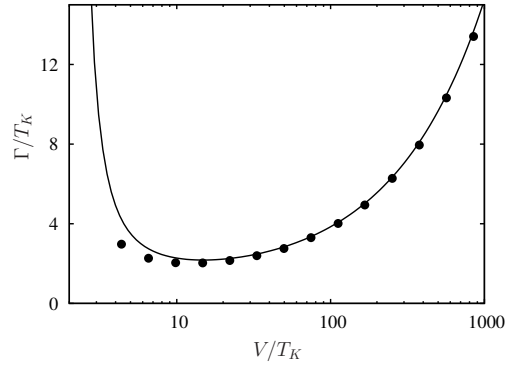


Fig. 7 Imaginary part of the self energy versus V/T_K . Dots: numerical results from FRG; solid line: $\Gamma = \frac{3}{4}V \frac{1}{(2 \ln(V=2T_K))^2}$.

in the regime $V \ll T_K$.

At finite voltage the charge current I_c is approximately given by

$$I_c = \frac{3}{2} \frac{e^2}{\hbar} \frac{d}{dV} \frac{d}{dV} \frac{d}{dV} \frac{d}{dV} \mathcal{G}(\omega; \omega; 0; 0) + \dots \quad (35)$$

:

In the limit of vanishing relaxation rate, the above expression simplifies to

$$I_c = \frac{3}{4} \frac{e^2}{\hbar} \frac{d}{dV} \mathcal{G}(\omega; \omega; 0; 0) \quad (36)$$

In Fig. 8 we show the conductance $G = I_c/V$ in units of G_0 as obtained from equ. (36) versus V/T_K at $T = 0$. Again, dots represent the numerical evaluation of the FRG equations, whereas the solid line represents an approximate analytical form $G = G_0 = \frac{3}{16} \frac{1}{\ln^2(V=2T_K)}$. One obtains this analytical result by replacing $g(\omega)$ by $g(\omega = 0)$ in equ. (32). However, because of the distinctive form of $g(\omega)$; which exhibits pronounced peaks at the resonance frequencies $\omega = \pm V=2$ the resulting $G(V) = G_0$ is slightly enhanced compared to the analytical form. In Fig. 9 results on the conductance $G = G_0$ versus V/T_K are presented for temperatures $T/T_K = 50; 10; 5$, such that one remains in the perturbative regime even in the limit $V \rightarrow 0$. Dots are the FRG results, whereas the solid line represents $G = G_0 = \frac{3}{4} g^2$ with the approximate vertex function

$$g(\omega = 0) = \frac{1}{2 \ln \frac{(V=2)^2 + T^2}{T_K}} \quad (37)$$

The frequency dependence of $g(\omega)$ together with the integration over the difference of the Fermi functions in the left and right lead in equ. (36) lead to a distinct discrepancy between the FRG result and the analytical form for $V \ll T$. In Fig. 10 results on G versus V/T_K in the same temperature regime as in Fig. 9 are shown. As can be seen, in the temperature range $3K \ll T \ll 10K$ saturates to a value of the order of T_K when the voltage falls below the corresponding temperature.

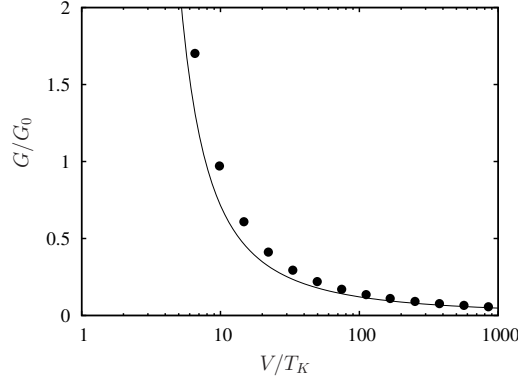


Fig. 8 Conductance $G = G_0 = I = V$ versus $V = T_K$. Dots: numerical result from FRG; solid line: $G = G_0 = \frac{3}{16} \frac{1}{\log^2(V=2T_K)}$.

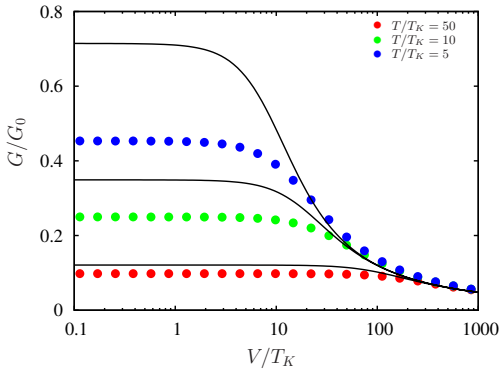


Fig. 9 Conductance in units of $G_0 = 2e^2/h$ as a function of $V = T_K$. Dots denote the result obtained by solving the fRG equations numerically. The solid line corresponds to the weak coupling form $G = G_0 = \frac{3}{16} \frac{1}{\log^2\left(\frac{(V=2)+T^2}{T_K}\right)}$.

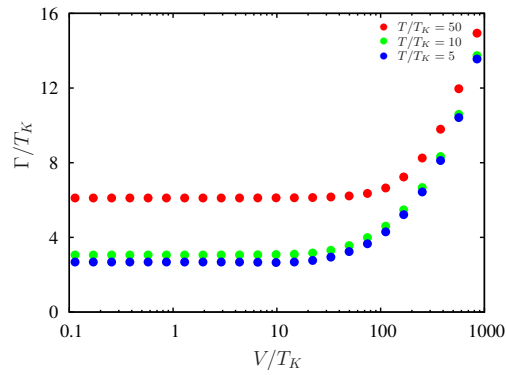


Fig. 10 Imaginary part of the self energy as a function of $V = T_K$. Dots represent again the results from the fRG.

3.5 Towards the strong coupling regime

From the previous considerations, i.e. the analysis and the solution of the approximated set of FRG equations 26, 27 and 28 it can be inferred that this set of equations in its present form is not appropriate to capture the physics in the strong coupling regime, i.e. in the regime $T \ll V = T_K$. There are two major deficiencies in the approximate RG equations: (1) the unitarity limit on the conductance, $G \leq G_0$ is not respected; (2) the spin relaxation rate Γ is found to rise with decreasing temperature/voltage in the strong coupling regime, whereas Γ is expected to saturate to a value of order T_K . There might be several reasons responsible for this failure.

First, the effect of higher order correlation functions is neglected in the approximation scheme discussed so far. The additional terms in the RG equation for the coupling function $g(l=0)$ generated thereby are similar, but not identical, to the higher order loop corrections to the poor man's scaling approach, and may be expected to slow down the growth of the coupling near the energy scale T_K . A quantitative control of these terms within FRG appears to be out of reach. Nonetheless, in the following we shall explore the

consequences of a model assumption including higher order terms. To this end we add terms of third and fourth order to the r.h.s. of equ. (26)

$$\text{Re } g = 2g^2 (1 - g^2) \tanh \frac{\omega}{2T} \frac{1}{\omega^2 + \Gamma^2}; \quad (38)$$

with coefficients α ; β to be determined by requiring that the unitarity limit be satisfied and that the resulting conductance fits the corresponding NRG result [29] best. We find that taking $\alpha = 0$ and putting $\beta = g_0^2 = 4/(3\pi)$, in equ. (38) leads to the best agreement with the NRG data on the linear response conductance [29]. Note that the additional terms are not interpreted as two-loop and three-loop contributions to the $\text{Re } g$ function. Rather, they are thought to represent the zero of the $\text{Re } g$ function at the strong coupling fixed point. A complete discussion of the $\text{Re } g$ function at equilibrium for the anisotropic Kondo model in the strong coupling regime has been given in [31], on the basis of the flow equation method. The simple ansatz used here cannot be compared with the entirely different approach of [31]. The point we want to make here is that a simple adjustment of the $\text{Re } g$ function for the coupling constant is not sufficient to capture the physics of the relaxation rate (see below).

In the following we keep the frequency dependence of $\text{Im } g$. Within the pseudo fermion projection scheme using the limit $\Gamma \ll T$ the self energy acquires a highly asymmetric form, which causes problems in the numerical solution. We therefore choose an alternative projection with $\Gamma = 0$ which requires to introduce normalization factors accounting for the difference in the impurity partition function with and without projection. In the calculation of $\text{Im } g$ in the absence of a magnetic field these factors are not necessary. This choice has the advantage of particle-hole symmetry, i.e. $\text{Im } g(\omega) = -\text{Im } g(-\omega)$.

The FRG equations (cf. 18, 21 and 24) then take the following form

$$\text{Re } g = g^2 (1 - (g-g_0)^2) \frac{\omega}{\omega^2 + \Gamma^2} \tanh \frac{\omega}{2T} \quad (39)$$

$$\text{Im } g = \frac{1}{2} \frac{\omega}{\omega^2 + \Gamma^2} \left[f(\omega) \mathcal{G}^>(\omega; T) + (1 - f(\omega)) \mathcal{G}^<(\omega; T) \right] \quad (40)$$

$$\text{Re } \mathcal{G}^>(\omega; T) = \frac{3}{4} g^2 \frac{\omega}{\omega^2 + \Gamma^2} \frac{(\omega + \tilde{\omega})}{(\omega + \tilde{\omega})^2 + \Gamma^2} (1 - f(\tilde{\omega})) \quad (41)$$

$$\text{Re } \mathcal{G}^<(\omega; T) = \frac{3}{4} g^2 \frac{\omega}{\omega^2 + \Gamma^2} \frac{(\omega + \tilde{\omega})}{(\omega + \tilde{\omega})^2 + \Gamma^2} f(\tilde{\omega}) \quad (42)$$

Fig. 11 shows a comparison of the linear conductance from FRG (dots) with the NRG data [29]. For the purpose of this comparison we adopted the definition of a Kondo temperature T_K used in [29]: $G(T_K) = G_0 = 2$. This differs from our previous definition of $T_K = D_0 \exp(-1/(2g))$ by a factor $T_K = T_K^{\text{old}} \cdot 2.76$. We find excellent agreement between the FRG and NRG results. In Fig. 12 we show the imaginary part of the pseudo fermion self energy ($\omega = 0$) as a function of $T = T_K$. The inset shows the region $T < T_K$, where $\text{Im } g$ again decreases almost linearly with decreasing temperature, down to a similar residual value of $\text{Im } g = T_K \approx 0.002$ as found from the weak coupling FRG equation above.

We now turn to the nonequilibrium situation: In Fig. 13 we show the conductance as a function of the voltage. The lines indicate the half width at half maximum which amounts to $V = 1.93 T_K$. Fig. 14 shows $\text{Im } g(\omega = 0)$ as a function of $V = T_K$. In the inset $\text{Im } g$ is seen to drop linearly with decreasing voltage at $V < T_K$, down to a residual value of $\text{Im } g = T_K \approx 0.002$.

To summarize, adding a fourth order term with adjusted coefficient to the $\text{Re } g$ -function of the RG equation for the coupling $g(\omega = 0)$ leads to good agreement with the exactly known conductance in the limit $V \gg 0$. The relaxation rate ($\omega = 0$), however, comes out three orders of magnitude too small. We conclude that

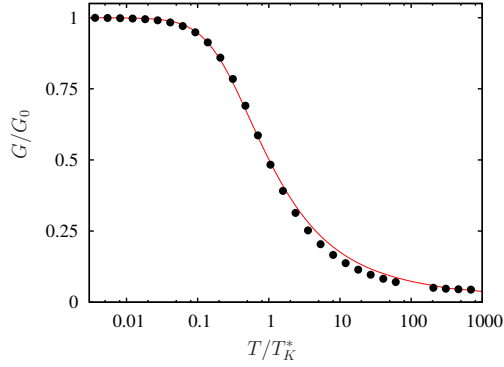


Fig. 11 Comparison of the linear conductance $G(T)$ from FRG (dots) with the result obtained via the NRG [29].

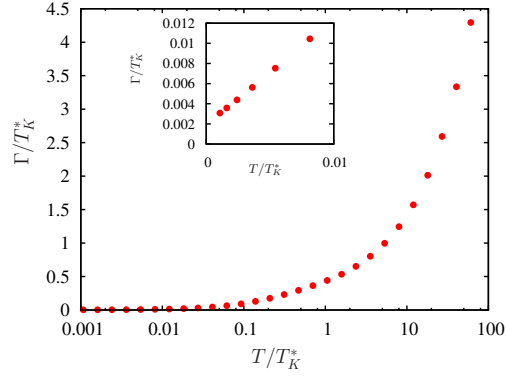


Fig. 12 Imaginary part of the pseudo fermion self energy ($\Gamma = 0$) versus of $T=T_K$ (note the logarithmic scale). Inset: Γ at $T=T_K = 1$ on a linear scale.

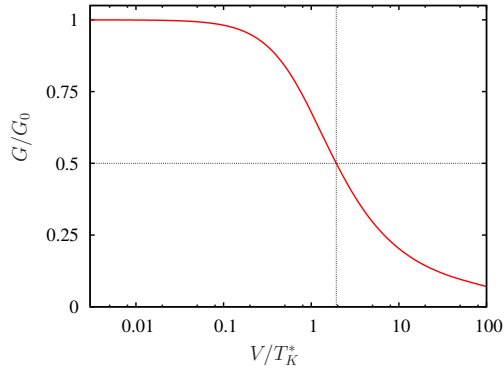


Fig. 13 Conductance $G(V)$ at $T = 0$ from FRG. The lines indicate the half width at half maximum which amounts to $V = 1.93T_K$.

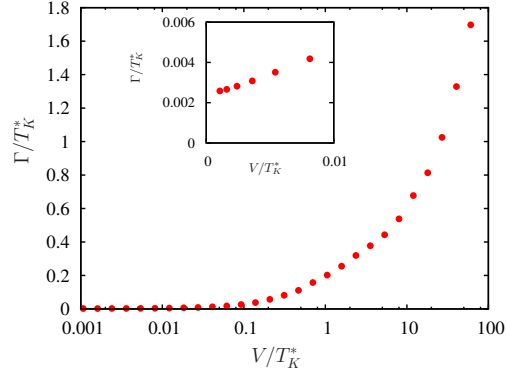


Fig. 14 Imaginary part of the pseudo fermion self energy ($\Gamma = 0$) versus $V=T_K$ on a logarithmic scale. Inset: Γ at $V=T_K = 1$ on a linear scale.

higher order terms in the γ -function are not sufficient to cure the problem with γ . In addition, the frequency dependence of both, γ and Γ is essential in reaching the Fermi liquid regime, as we now sketch.

First we note that unitarity does not require $\gamma(\omega)$ to be bounded at all frequencies. It appears possible to have $\gamma(\omega = 0)$ growing large or even diverging at strong coupling, while the conductance G remains finite. This is because G as given by equ. (35) is given by integrating the product of two γ 's over energy. The energy integration removes any singular behavior of γ at $\omega = 0$ provided the singularity is not too strong.

Secondly, a sufficiently strong relaxation rate Γ might suppress the unphysical growth of γ . As discussed in detail in section 3.3 the RG equations in the approximation of taking all energies on shell do not generate a sufficiently strong $\gamma(\omega = 0)$ at the scale $\omega = T_K$, where it would be needed to cut off the growth of γ , for the reasons discussed above. On the other hand, γ at $\omega = 0$ turned out to grow too large at $T = T_K$. This deficient behavior may also be remedied by taking the energy dependence of Γ and γ into account. Qualitatively one expects that the smearing of the sharp singular structures in $\gamma(\omega)$ and $\Gamma(\omega)$ by integrations over ω' within the width Γ specified by the pseudofermion spectral functions will be equivalent to replacing $\gamma(\omega = 0)$ and $\Gamma(\omega = 0)$ by $\gamma(\omega = \Gamma)$ and $\Gamma(\omega = \Gamma)$, which are both finite quantities of $\mathcal{O}(1)$ and $\mathcal{O}(T_K)$, respectively, not only at the end of the RG process (at $\omega = 0$), but already at $\omega = T_K$.

4 Conclusion and outlook

With the advent of nanophysics in the mid 1990s it became possible to fabricate nanostructures with the properties of single atoms. In contrast to real atoms these artificial atoms may be contacted by metallic leads, opening a new way of probing their properties in transport measurements. This development led to a revival of Kondo physics, a subject that had emerged in studies of dilute magnetic alloys. Even though the Kondo effect had been well understood by the mid 1970s, the new development required theories describing the Kondo effect out of equilibrium. Most of the theoretical methods created to describe the Kondo effect in equilibrium do not work or work only in a limited way for systems out of equilibrium. A good starting point is perturbation theory in the Keldysh formulation. However, due to the infrared singular behavior of the Kondo problem, simple perturbation theory is not sufficient. In equilibrium the powerful method of the renormalization group has been proposed and successfully implemented first by Anderson in the perturbative regime and later by Wilson, all the way to strong coupling.

Anderson's perturbative treatment has been generalized to non-equilibrium in [10, 11], after recognizing two important new features. First, in nonequilibrium the coupling constant has to be generalized to an energy dependent coupling function. Second, the processes limiting the quantum coherence of the allimportant spin flip processes that are responsible for the Kondo effect in the first place, become more important out of equilibrium and may stop the RG flow to strong coupling inside the weak coupling regime. The latter lead to a decoherence rate, which in [10, 11] was added ad hoc to the RG equations. In the present paper the decoherence rate is treated from the beginning on equal footing with the coupling function. It is known [30] that the decoherence rate is given by the physical spin relaxation rate. In technical terms, the spin relaxation rate has contributions from the self energy as well as from vertex corrections. Within the standard quantum field theoretical formalism used in this paper, it is straightforward to incorporate the self energy contribution. To include the vertex corrections would require to take into account three particle processes as well. The latter are beyond the scope of what has been done in the present paper. There exist different formulations based on the Liouville operator formalism [33] or the flow equation method [32], which allow to take into account vertex corrections in a systematic way. However, these methods have their own drawbacks. The main achievement of the present paper is therefore the principal demonstration of the appearance and the actual calculation of the effect of the decoherence rate on the RG flow for the Kondo model.

It is tempting to explore the importance of the decoherence processes in cutting off the RG flow to strong coupling in equilibrium, where it is strongest. From the known behavior of the spin relaxation rate as a function of temperature one would expect that at temperatures at and below the Kondo temperature the RG flow is already cut off and the coupling constant would tend to a temperature independent value with T^2 -corrections at low T . We found something different: apparently the coupling function $g(\omega = 0)$ grows to values much larger than unity, without, however, violating the unitarity limit. A careful solution of the frequency dependent RG equations is a subject for future work. If the coupling grows to large values one should expect higher order processes to become important. We have added higher order terms to the RG equation, in such a way that $g(\omega = 0)$ tends to a finite value of order unity, recovering the unitarity limit of the conductance in its simplest form. The resulting conductance curve is in good agreement with NRG results known for the equilibrium case, and allows to explore the behavior at finite bias voltage.

5 Acknowledgement

We are grateful to Hans Kroha and Achim Rosch for useful discussions in the early stages of this work. Special thanks are owed to Jens Paaske for discussions on many aspects of RG in the Kondo problem.

References

- [1] W. G. van der Wiel, S. de Francheschi, J. M. Elzerman, T. Fujisawa, S. Tarucha and L. P. Kouwenhoven, *Rev. Mod. Phys.* **75**, 1 (2003).
- [2] D. Goldhaber-Gordon et al., *Nature* **391**, 156 (1998).
- [3] S. M. Cronenwett et al., *Science* **281**, 540 (1998).
- [4] W. G. van der Wiel et al., *Science* **289**, 2105 (2000).
- [5] J. Nygard et al., *Nature* **408**, 342 (2000).
- [6] T. S. Jespersen et al., *Phys. Rev. B* **74**, 2333304 (2006).
- [7] A. Rosch, J. Kroha and P. Wölfle, *Phys. Rev. Lett.* **85**, 156802 (2001).
- [8] A. Kaminski, Yu. V. Nazarov and L. I. Glazman, *Phys. Rev. Lett.* **83**, 384 (1999); *Phys. Rev. B* **62**, 8154 (2000).
- [9] P.W. Anderson, *J. Phys. C* **3**, 2436(1970).
- [10] A. Rosch, J. Paaske, J. Kroha and P. Wölfle, *Phys. Rev. Lett.* **90**, 076804 (2003).
- [11] A. Rosch, J. Paaske, J. Kroha and P. Wölfle, *J. Phys. Soc. Jpn.* **74**, 118 (2005).
- [12] J. Paaske, A. Rosch, P. Wölfle, N. Mason, C. M. Marcus and J. Nygard, *Nature Physics* **2**, 460 (2006).
- [13] V. Koerting, P. Wölfle and J. Paaske, *Phys. Rev. Lett.* **99**, 036807 (2007).
- [14] V. Koerting, J. Paaske and P. Wölfle, *Phys. Rev. B* **77**, 165122 (2008).
- [15] S. Kehrein, *Phys. Rev. Lett.* **95**, 056602 (2005)
- [16] A. C. Hewson, *The Kondo effect to Heavy Fermions* (Cambridge University Press, 1988).
- [17] S. Kirchner, J. Kroha and P. Wölfle: *Phys. Rev. B* **70**, 165102 (2004).
- [18] J. Kroha and P. Wölfle, *J. Phys. Soc. Jpn.* **74**, 16 (2005).
- [19] C. Wetterich, *Phys. Lett. B* **301**, 90 (1993).
- [20] M. Salmhofer, *Renormalization: An Introduction* (Springer, Berlin, 1998).
- [21] V. Meden, in *Advances in Solid State Physics* **46**, ed. R. Haug (Springer, New York, 2007).
- [22] W. Metzner, *Functional renormalization group approach to interacting Fermi systems*, *Lecture Notes in Physics* (Springer, Berlin, 2007).
- [23] Jakobs, V. Meden and H. Schoeller, *Phys. Rev. Lett.* **99**, 150603(2007).
- [24] D. Schuricht and H. Schoeller, *Phys. Rev. B* **80**, 075120 (2009).
- [25] A.A. Abrikosov, *Physics* **2**, 5 (1965).
- [26] J. Paaske, A. Rosch and P. Wölfle, *Phys. Rev. B* **69**, 155330 (2004).
- [27] J. W. Negele, and H. Orland, *Quantum Many-Particle Systems*, Addison-Wesley (1988).
- [28] J. Rammer and H. Smith, *Rev. Mod. Phys.* **58**, 323 (1986).
- [29] R. Bulla, T. Pruschke and T. Costi, *Rev. Mod. Phys.* **80**, 395 (2008).
- [30] J. Paaske, A. Rosch, J. Kroha, and P. Wölfle, *Phys. Rev. B* **70**, 155301 (2004).
- [31] W. Hofstetter and S. Kehrein, *Phys. Rev. B* **63**, 140402(R) (2001).
- [32] P. Fritsch and S. Kehrein, *Annals of Physics* **324**, 1105 (2009).
- [33] H. Schoeller, *Eur. Phys. J. Special Topics* **168**, 179 (2009).